University of Baghdad
College of Engineering
JOURNAL OF ENGINEERING

# Journal of Engineering

journal homepage: www.joe.uobaghdad.edu.iq
Number 10 Volume 24 October 2018

***Civil and Architectural Engineering***

# Finite Element Analysis of Raft Foundation under Coupled Moment

**Dr. Faris Waleed Jawad***
Ministry of Higher Education and Scientific Research / Department of Reconstruction and Projects
civileng_faris@yahoo.com

## ABSTRACT

Due to wind wave actions, ships impacts, high-speed vehicles and others resources of loading, structures such as high buildings rise bridge and electric transmission towers undergo significant coupled moment loads. In this study, the effect of increasing the value of coupled moment and increasing the rigidity of raft footing on the horizontal deflection by using 3-D finite element using ABAQUS program. The results showed that the increasing the coupled moment value leads to an increase in lateral deflection and increase in the rotational angle (α◦). The rotational angle increases from (0.014, 0.15 to 0.19) at coupled moment (120 kN.m), (0.29, 0.31 and 0.49) at coupled moment (240 kN.m) and (0.57, 0.63 and 1.03) at coupled moment (480 kN.m) with decreasing the raft thickness from (1.5, 1.0 to 0.5m), respectively. The computed maximum lateral deflection decreases with increasing the rigidity of raft. The maximum deflection decreases from (40 to 3mm) at coupled moment 120 kN.m, (150 to 60mm) at coupled moment 240 kN.m and (210 to 118mm) at coupled moment 480 kN.m with increase raft thickness from (t = 0.5 to 1.5m) and the maximum reduction in maximum stress value and lateral deflection mobilized due to applied coupled moment is noticed when width to thickness of footing ratio is less than (w/t<12). The failure of the footing is noticed when the rotational angle is more than 4° ($\alpha > 4^{\circ}$)

**Keywords:** Raft foundation; rigidity; rotational angle; coupled moment; numerical analysis.

# تحليل بالعناصر المحددة للاسس الحصيرية تحت تاثير العزم المزدوج

**د.فارس وليد جواد**
وزارة التعليم العالي والبحث العلمي / دائرة الاعمار والمشاريع

## الخلاصة

نتيجة للاحمال الناتجة من تاثير الريح والسفن والسرعة الفائقة للمركبات احمال اخرى ذات مصادر مختلفة فان المنشاءات متعددة الطوابق والجسور وابراج نقل الطاقة الكهربائية تكون تحت تاثير العزم المزدوج. البحث ياخذ بنظر الاعتبار تاثيروقيمة العزم المزدوج والجساءة للاساس الحصيري وتاثيرهما على الاود الجانبي للاساس باستخدام العناصر المحددة المتاحة في برنامج (ABAQUS) . النتائج تظهر ان زيادة العزم المزدوج يؤدي الى زيادة الاود الجانبي للاساس الحصيري وزيادة في زاوية الدوران الاساس (α◦). ان زاوية الدوران تزداد من (0.14 الى 0.19) عندما العزم المزدوج (120 kN.m)،(0.29 الى 0.49) عندما العزم المزدوج (240 kN.m) ومن (0.57 الى 1.03)عندما العزم المزدوج (480 kN.m) بتقليل سمك الاساس من(1.5 الى 0.5)على التوالي. وان الاود الجانبي لاساس يقل بزيادة جسائة الاساس برغم من زيادة قيمة العزم المزدوج حيث تقل من (40 الى 3 ملم) عند العزم المزدوج (120 kN.m)، (150 الى 60 ملم) عند العزم المزدوج (240kN.m) و (210 الى 118 ملم) عندالعزم المزدوج (480 kN.m) مع زيادة سمك الاساس من 0.5 الى 1.5 على التوالي. عندما تكون نسبة عرض الاساس الى سمكه اكبر من 12 نلاحظ اعظم نقصان بالاود الجانبي للاساس والاجهادات المتولدة نتيجة لتاثير العزم المزدوج. ان حالة فشل الاساس تظهر عندما تكون زاوية الدوران اكبر من 4°.

**الكلمات الرئيسية**:اساس حصيري، الجسائة، زاوية الدوران، العزم المزدوج، تحليل عددي

*Corresponding author
Peer review under the responsibility of University of Baghdad.
https://doi.org/10.31026/j.eng.2018.10.06

Article accepted: 9/1/2018

## 1. INTRODUCTION

The disposal of a laterally loaded footing has been examined for over 40 years. Many researchers have contributed to this area in different ways (e.g. field tests, model tests, centrifuge tests analytical solution, and numerical analysis). Several numerical analysis methods for example boundary element method and finite element method have been adopted. The previous researchers such as **Spillers** and **Stoll, 1964, Douglas** and **Davis, 1964**, **Poulos, 1971,** and **Banerjee** and **Davies, 1978,** showed the solutions to the displacement and rotation of a thin vertical rigid plate with lateral load and bending moment. When the soil is represented by a stiffness of the elastic spring, in other words, the soil is represented by the modulus of lateral subgrade reaction. The earliest to use the springs represent the interaction between soil and foundation, **Winkler, 1867,** showed the solutions of the equation are available for modulus of elasticity constant with depth. **Hetenyi, 1964,** presented the solutions of the modulus of elasticity varying linearly with depth **Reese** and **Matlock, 1956** and **Davisson** and **Gill, 1963,** showed the solutions of layered systems

In this paper the effect of changing the value of coupled moment for (raft footing–soil stiffness) resting on loose sand was studied, the 3-D finite element analyses were carried out using **ABAQUS/CAE 6.10.1** program.
The parameters studied were:

1- Coupled moment values (120, 240 ,480 kN.m)
2- Raft thickness (t= 0.5, 1.0 and 1.5m) and the width of the footing to the thickness ratio become as (w/t = 24, 12 and 8).

## 2. DEFINITION OF MOMENT OF COUPLE

**Hibbeler, 2004,** stated that the couple defined as the two parallel forces have the same magnitude but opposite directions, and separated by a vertical distance (d), as shown in **Fig. 1.** Since the resultant force is zero, the only effect of a couple which results in a rotation or tendency of rotation in a specified direction and the couple moment is produced by a couple. The value of coupled moment can be defined by Eq. (1).

$$M=f\ x\ d \tag{1}$$

The idealization of couple moment and forces applied to the raft foundation model is illustrated in **Fig. 2.**

## 3. FAILURE CRITERIA

For footing loaded laterally, the failure criterion is very important because it is usually less than from footing loaded vertically. Many researchers have illustrated that the failure criteria of the settlement are 10% of the width of footing, **Jawad, 2009**. The footing is loaded under the coupled moment, no clear failure criteria can be listed, while the rotational angle of raft footing or lateral deflection may happen due to loading the footing may be considered as the limited value for failure.

## 4. INPUT PARAMETER IN ABAQUS

The behavior of square raft materials and sand soil are assumed to be a linear elastic material during the 3-D analysis and the properties of raft foundation and sand materials are listed in **Tables 1 and 2**, respectively.

## 5. BEHAVIOR OF MATERIAL IN ABAQUS

The 3-D generalized Hooke's law is favorite for isotropic linear elastic materials in 3-D stress conditions. Hooke's law is used to estimate the elastic strains associated with applied stresses within a raft mass have isotropic materials which mean that the coefficients of elastic moduli, such as (E, Young's modulus) and (ν, Poisson's ratio) are included in calculations. The Drucker-Prager was used to describe the behavior of sandy soil in which the yield behavior depends on the equivalent pressure stress. The inelastic deformation of sand soil sometimes is associated with frictional mechanisms such as sliding of particles across each other.

## 6. FINITE ELEMENT EQUATIONS

The state of stresses with any point in the mass of soil is represented by a very small cube with three stress components on each of its six sides (one normal and two shear components) as shown in **Fig. 3**. The strain is known as the change of displacement per unit length and the components of strain can be explained by driving of the displacements to the original length as illustrated by **Liu** and **Quek, 2003**.

$$\varepsilon_x = \frac{\partial(u)}{\partial(x)} \quad . \; \varepsilon_y = \frac{\partial(v)}{\partial(y)} \qquad \varepsilon_z = \frac{\partial(w)}{\partial(z)}$$

$$\varepsilon_{(xy)} = \frac{\partial u}{\partial y} + \frac{\partial v}{\partial x} \quad \varepsilon_{(xz)} = \frac{\partial u}{\partial z} + \frac{\partial w}{\partial x} \quad \varepsilon_{(yz)} = \frac{\partial v}{\partial z} + \frac{\partial w}{\partial y} \tag{2}$$

Whereas *u*, *v* and *w* are the components of displacement in x, y and z directions, respectively. **Eq. (2)** above which show six strain–displacement relationships can be written in the formula of the matrix:

$$\varepsilon = (L) \, . \, (U) \tag{3}$$

Where U, is the vector of the displacement vector and has been produced from.

$$(U) = \begin{Bmatrix} (u) \\ (v) \\ (w) \end{Bmatrix} \tag{4}$$

And L is a matrix of partial differential

$$\mathbf{L}=\begin{bmatrix} (\partial/\partial x) & 0 & 0 \\ 0 & (\partial/\partial y) & 0 \\ 0 & 0 & (\partial/\partial z) \\ 0 & (\partial/\partial z) & (\partial/\partial y) \\ (\partial/\partial z) & 0 & (\partial/\partial x) \\ (\partial/\partial y) & (\partial/\partial x) & 0 \end{bmatrix} \quad (5)$$

## 7. NUMERICAL ANALYSIS

All the numerical calculations were made by the finite element program **ABAQUS/CAE.** The 3D-models were configured for the dimension of the soil and the foundation and each soil and foundation properties were taken in the model.

The disposal of raft foundation was represented by linear elastic and the soil behavior was considered the linear elastic model. In **ABAQUS/CAE** program a mesh of model type **C3D8R** and 8-node linear hexahedral element were used and the total numbers of elements were (24392) as shown in **Fig. 4.** The interactions between the base footing and soil were taken into account, in order to define the properties of attraction in the program the movement between footing and soil was considered a normal and a kind of attraction between the raft and soil was rough to represent the full adhesion between the two surfaces.

## 8. STEPS, APPLIED LOADS AND BOUNDARY CONDITIONS

The armed forces are static forces, which are placed at the two edges of the footing; the distance between them is vertical. The boundary conditions in the program were defined so as to prevent movement in the z-direction. **Fig. 5** describes the idealization of load and boundary conditions.

## 9. RESULTS AND DISCUSSION OF NUMERICAL WORKS

**Figs 6 to 8** show the lateral deflection at the edge of the footing in the node where the forces were applied with coupled moment curves resulting from the applied variable value of parallel forces at the edge of footing when raft thickness is variable from (0.5, 1.0 and 1.5m). In general, the results show that the increase in coupled moment value leads to increase in lateral deflection and the rotational angle ($\alpha^{\circ}$) which is defined as tan for the percentage of lateral deflection ($\Delta$) divided by the perpendicular size of raft footing (w).

$$\tan\alpha=\frac{\Delta}{w} \quad (6)$$

The rotational angle increases from (0.014, 0.15 to 0.19) at coupled moment (120 kN.m), (0.29, 0.31 and 0.49) at coupled moment (240 kN.m) and (0.57, 0.63 and 1.03) with decrease in raft thickness from (1.5, 1.0 to 0.5m), respectively. From above figures, a value of the angle of rotational footing at failure is more than $4^{\circ}$. **Fig. 9** shows that the computed maximum lateral deflection decreases when the rigidity of raft increases. It can be noticed that the increase in raft thickness about (2t) has great influence on decreasing the value of maximum lateral deflection, while the lateral deflection value does not change significantly when the thickness of raft footing increases from (2t) to (3t). The maximum lateral deflection decreases from (40 to 3mm) at coupled moment 120 kN.m, (150 to 60mm) at the coupled moment 240 kN.m and (210 to 118mm) at coupled moment 480 kN.m with increase in raft thickness from (t = 0.5 to 1.5m),

respectively. It can be concluded from the above results that to reduce the lateral deflection the width to thickness ratio should become less than (w/t < 12). **Figs. 10, 11 and 12** show the computed stress in the x-direction along the size of the raft in the perpendicular direction of applied loads. The response of stress will increase with increasing the value of coupled moment applied on the surface of footing. The stress will be decreased from (840, 410 to 180 kPa), (860, 430 to 210 kPa) and (660, 320 to 160 kPa) at raft thickness increase from (0.5, 1.0 to 1.5m), respectively. **Fig. 13** shows the increase in the raft thickness to (2t) has no effect on the maximum stress will be mobilized in the raft due to applied coupled moment, while when increasing the raft thickness to (3t) it is noticed that the reduction in maximum stress value becomes more clear, in other words, the ratio of width of footing to thickness becomes less than (w/t < 12).

## 10. VISUALIZATION OF NUMERICAL WORKS

The results obtained from the program have been presented and the visualization of deflection displayed can be seen in **Figs. 14 to 19,** where the three-dimensional full contour mapping of lateral deflection for varied coupled moment and raft thickness are shown.

## 11. CONCLUSIONS

1- In general, the increase in coupled moment value leads to increase in lateral deflection and increases in the rotational angle ($\alpha^{\circ}$)
2- Lateral deflection decreases when the rigidity of raft increases, in order to ensure minimum lateral deflection, the footing width to thickness ratio should be less than (12).
3- The response of stress will increase with the increase in the value of coupled moment applied on the surface of the footing
4- The stress decreases when the raft thickness increases and the least value of the stress mobilized by the applied coupled moment is when the width to thickness ratio is less than (12).
5- At failure, the angle of the rotational footing is more than $\alpha > 4^{\circ}$

## 12. REFERENCES


- Banerejee, P.K., and Davies, T. G., 1978, *The Behavior of Axially and Laterally Loaded Single Piles Embedded in Nonhomogeneous Soils*, Geotchnique, 28 (3): 309-326.
- Davission, M. T., and Gill, H. L., 1963, *Laterally Loaded Piles in Layered Soil System*, Journal of the Soil Mechanics and Foundations, Division, ASCE, 89 (3): 63-94.
- Douglas, D. G., and Davies, E. H., 1964, *The Movement of Buried Footing due to Moment and Horizontal Loads and The Movement of Anchor Plates*, Geotechnique, 14:115-123.
- Hetenyi, M., 1964, *Beams on Elastic Foundations, University of Michigan Press*, Ann Arbor, Michigan.
- Hibbeler, R. C., 2004, *Engineering Mechanics Statics*, third addition person education South Asia Pte Ltd**.**
- Jawad, F. W., 2009, *Improvement of Loose Sand Using Geogrids to Suport Footing Subjected to Eccentric Loads*, M.Sc. Thesis, and Baghdad University.
- Liu, G. R., and Quek, S. S., 2003, *The Finite Element Method: A Practical Course*, Book, Elsevier Science Ltd**.**
- Poulus, H.G., 1971, *Behavior of Laterally Loaded Piles:1-Single Piles*, Journal of the Soil Mechanics and Foundations Division, ASCE, 97(5):711-731.

- Reese, L. C., and Matlock, H., 1956, *Non-dimensional Solutions for Laterally Loaded Piles with Soil Modulus Assumed Proportional to Depth*, In proceeding of the 8th Texas Conference on Soil Mechanics and Foundations Engineering, Austin, Texas, PP. 1-25.
- Spillers, W. R., and Stoll, R. D., 1964, *Lateral response of Piles*, Journal of the Soil Mechanics and Foundations Division, ASCE, 90(6):1-9.
- Winkler, E., 1867, *On Elasticity and Fixity*, H. Dominicus, Prague in German.


## 13. SYMBOLS

d= vertical distance between forces, m.
f= force, m.
t= thickness of raft, m.
u= displacement in x-direction, m.
v= displacement in y-direction, m.
w= displacement in z-direction, m.

$\varepsilon_x$ = strain in x-direction
$\varepsilon y$ = strain in y-direction
$\varepsilon z$ = strain in y-direction
$\varepsilon xy$ = strain in xy-directions
$\varepsilon xz$ = strain in xz-directions
$\varepsilon yz$ = strain in yz-directions

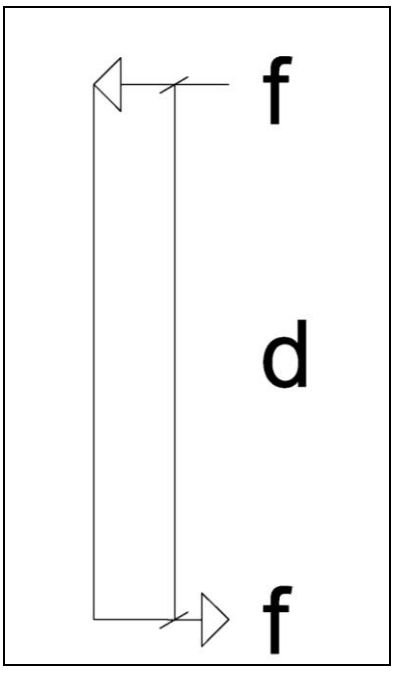


**Figure 1.** Definition of the coupled moment, **Hibbeler, 2004**.

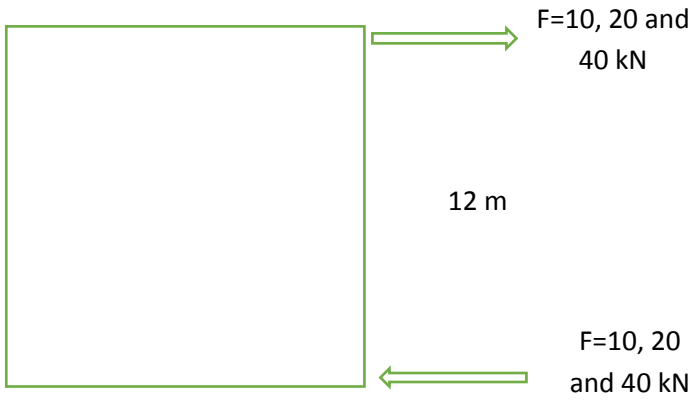


**Figure 2**. Top view of raft footing and points of applied loads.

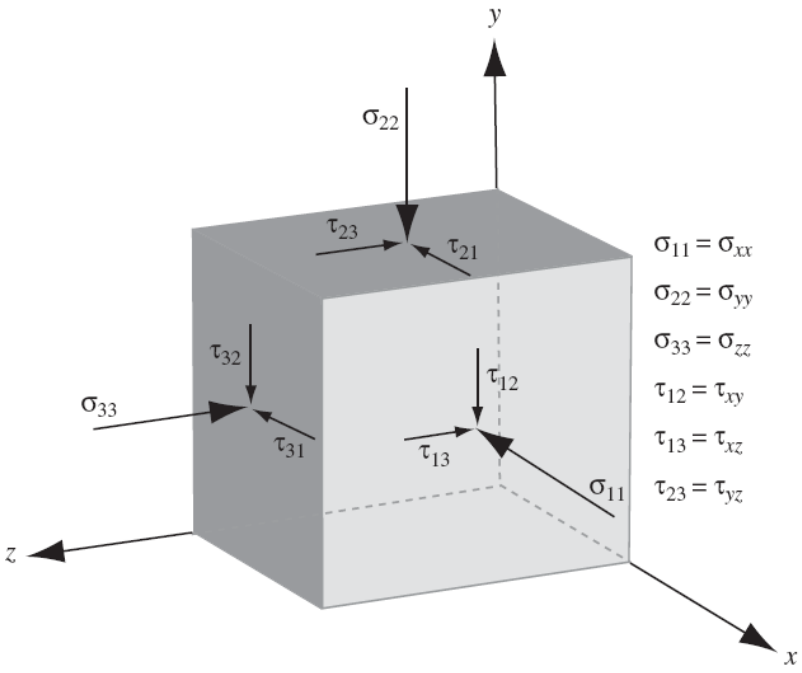


**Figure 3**. Stresses in three dimensional element**.**

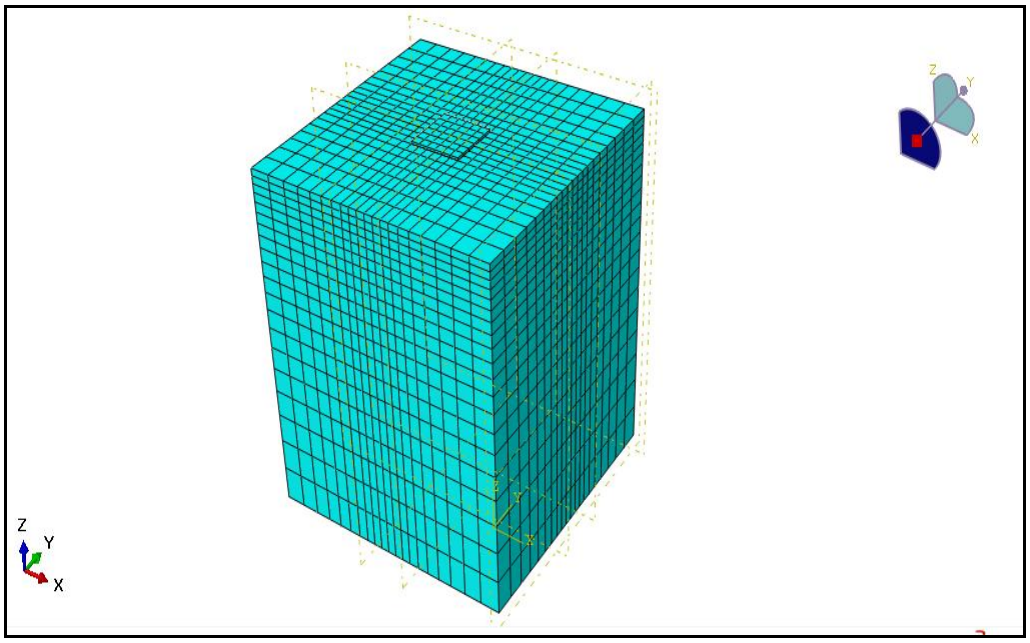


**Figure 4**. Meshing model of the raft with soil.

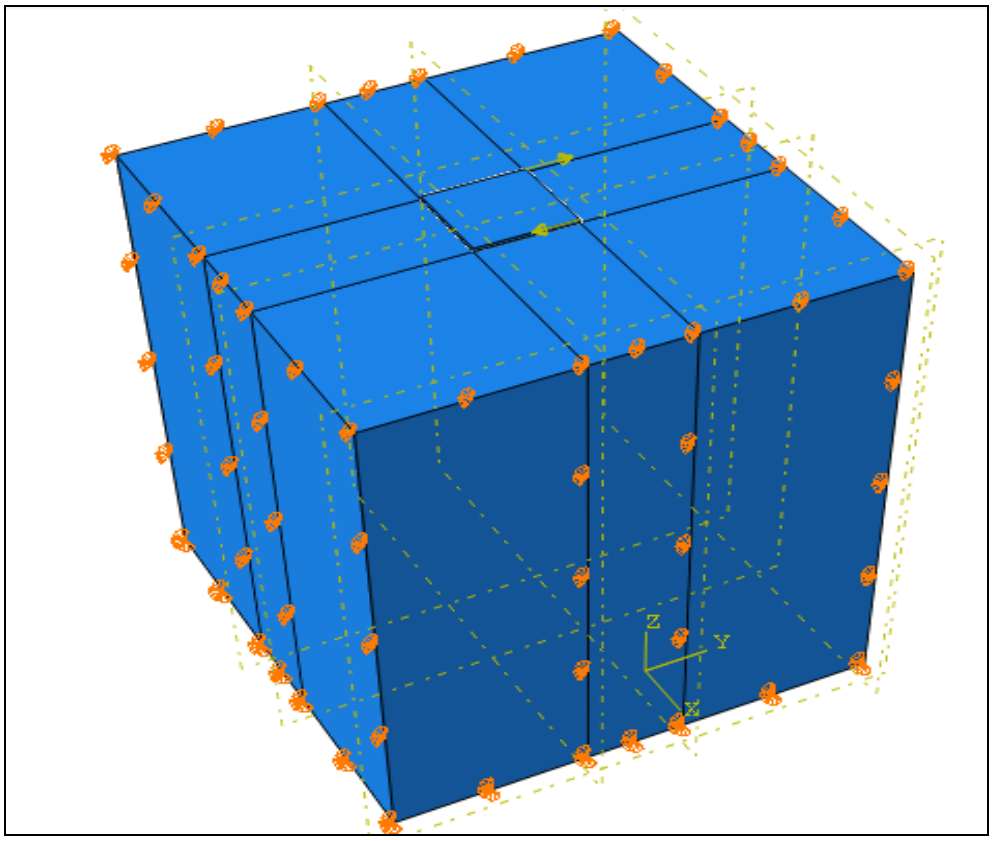


**Figure 5**. The load applied and boundary conditions.

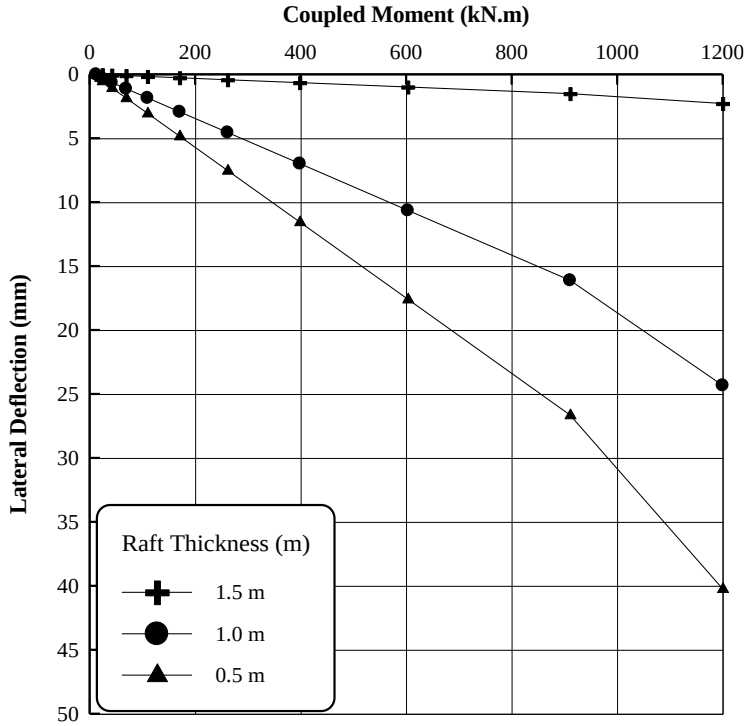


**Figure 6.** Coupled moment versus deflection in the node where the forces were applied (F=10 kN).

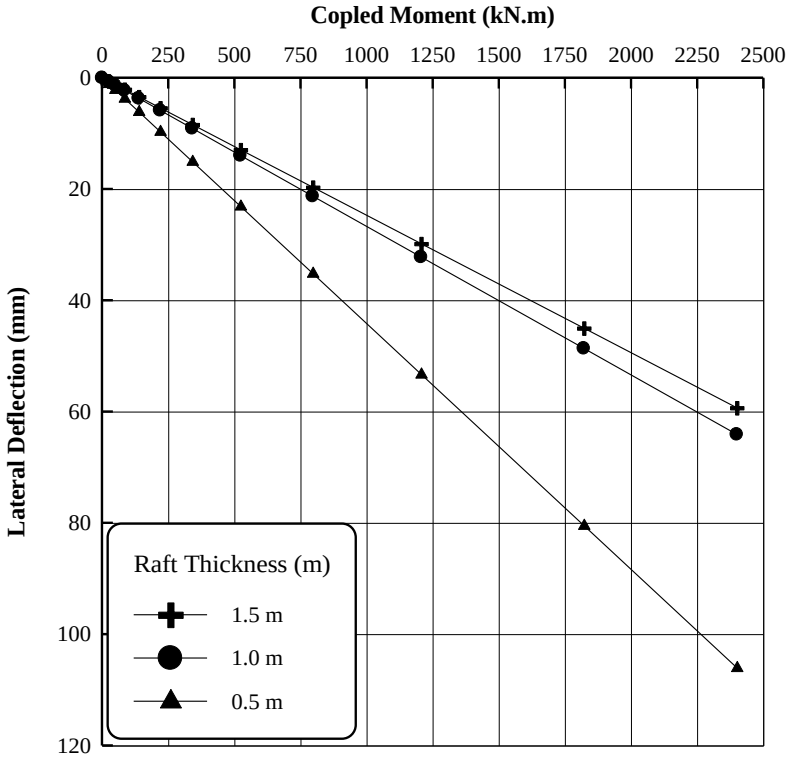


**Figure 7.** Coupled moment versus deflection in the node where the forces were applied (F=20 kN).

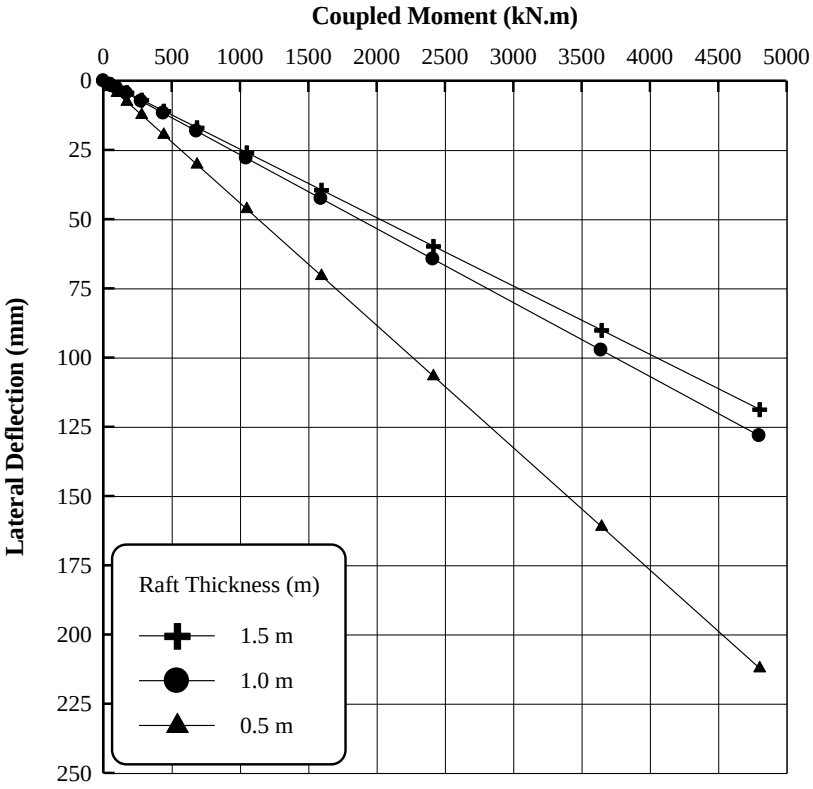


**Figure 8.** Coupled moment versus deflection in the node where the forces were applie**d** (F=40 kN).

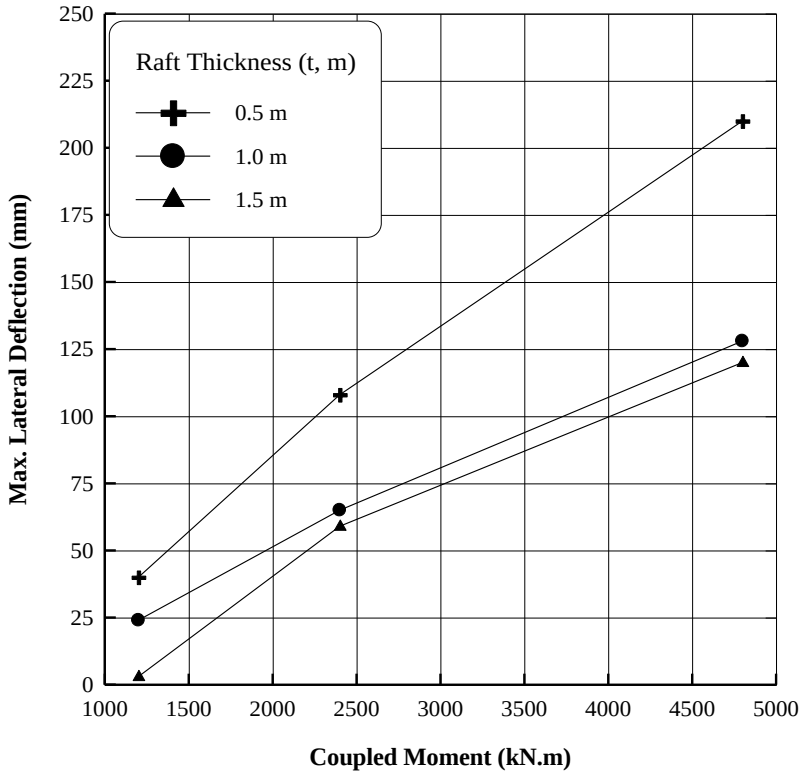


**Figure 9.** Coupled moment versus max deflection for different raft thickness.

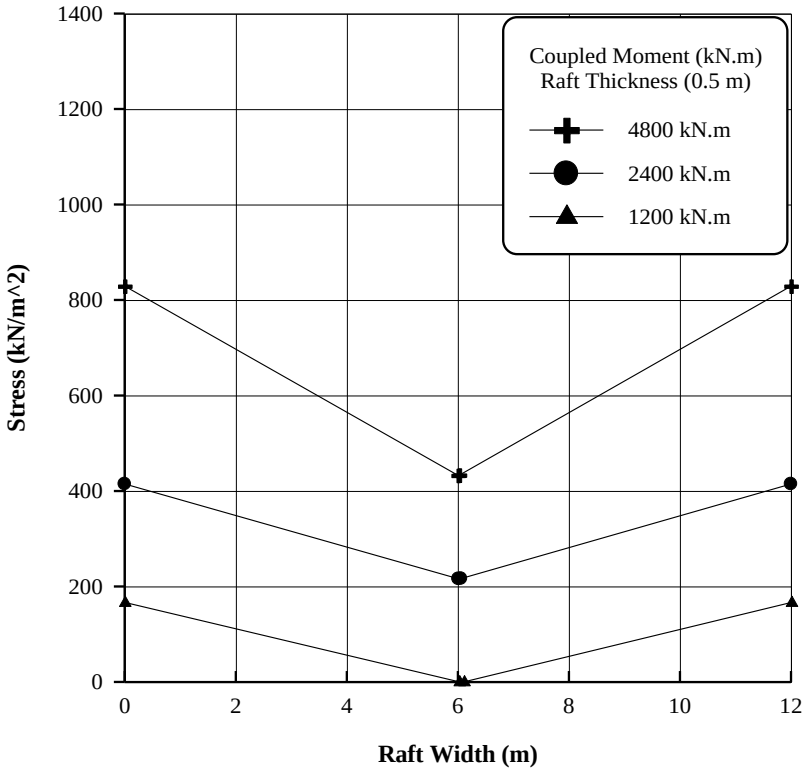


**Figure 10.** The distribution of stresses along raft width in the x-direction at (raft thickness=0.5m).

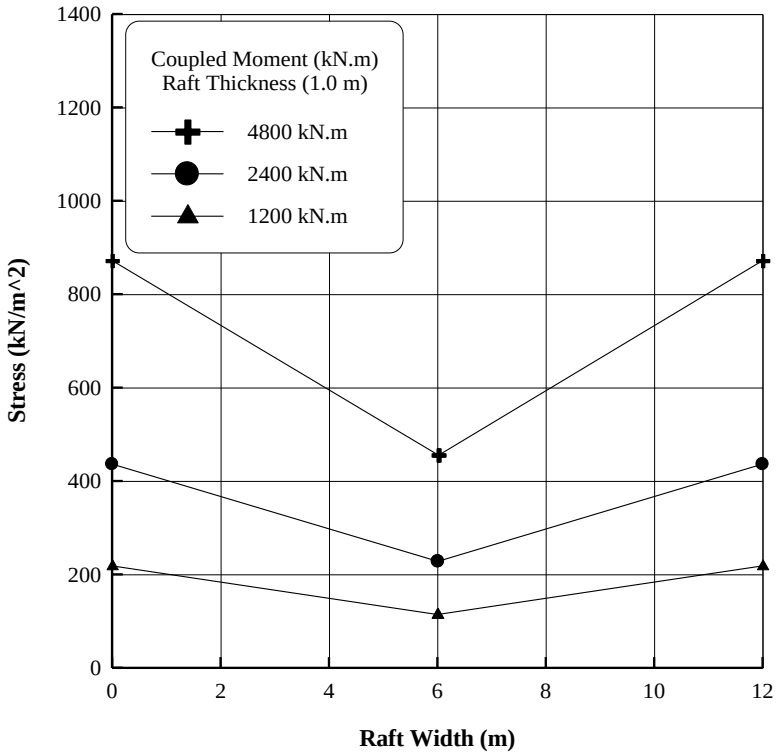


**Figure 11.** The distribution of stresses along raft width in the x-direction at

(raft thickness=1.0 m).

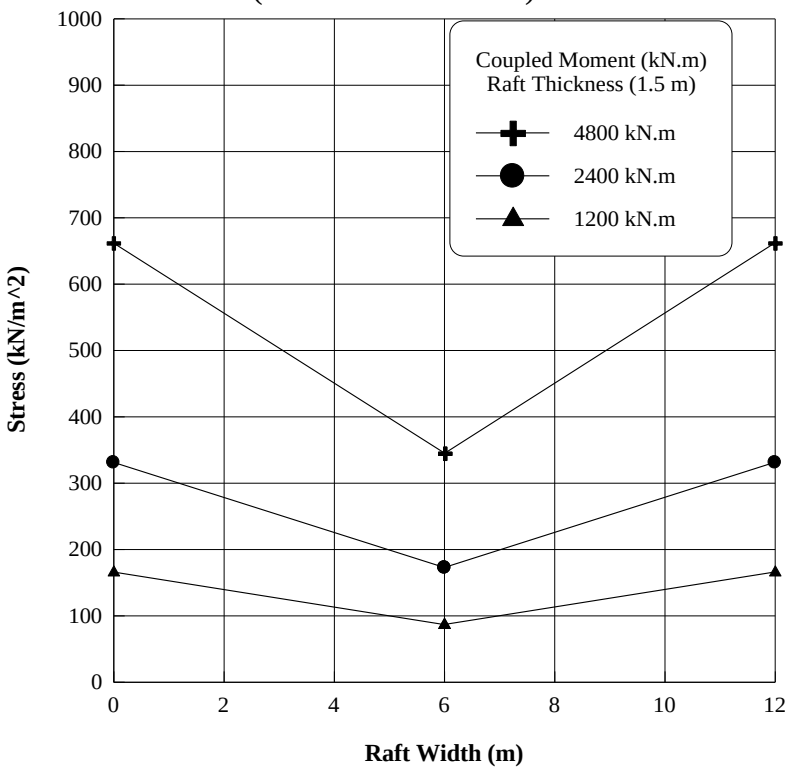


**Figure 12**. The distribution of stresses along raft width in the x-direction at (raft thickness=1.5m).

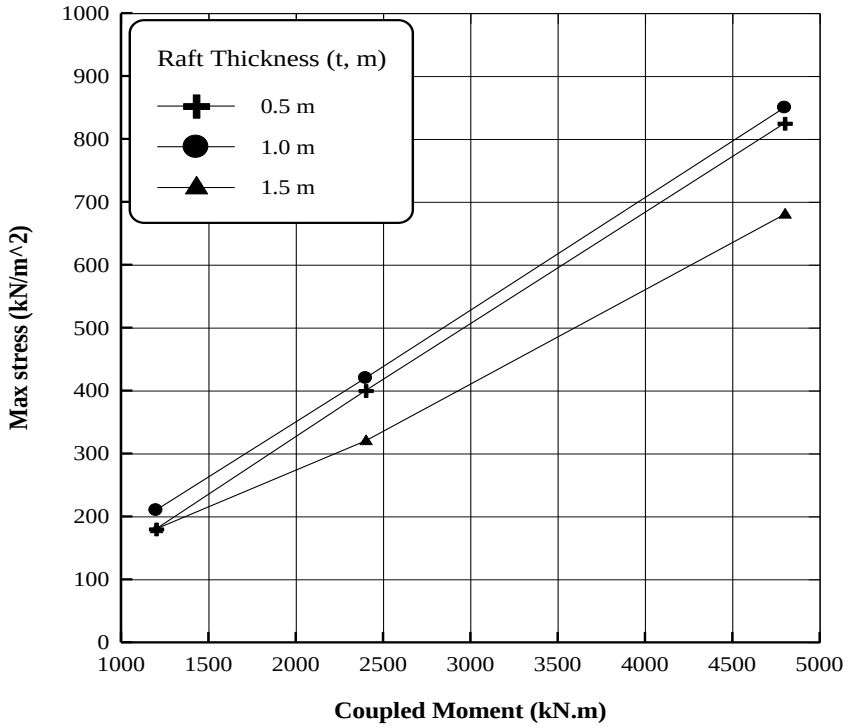


**Figure 13.** Max. Stresses in the x-direction versus coupled moment**.**

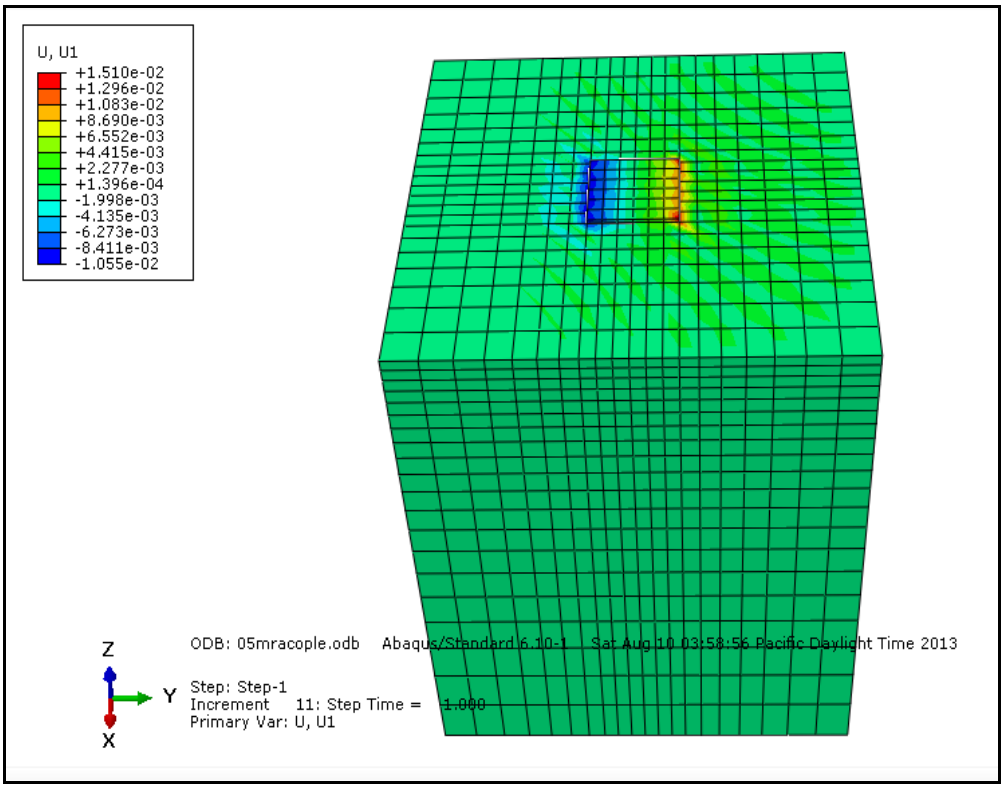


**Figure 14.** Full contours of lateral deflection (m) at raft thickness = 0.5m and F=10 kN.

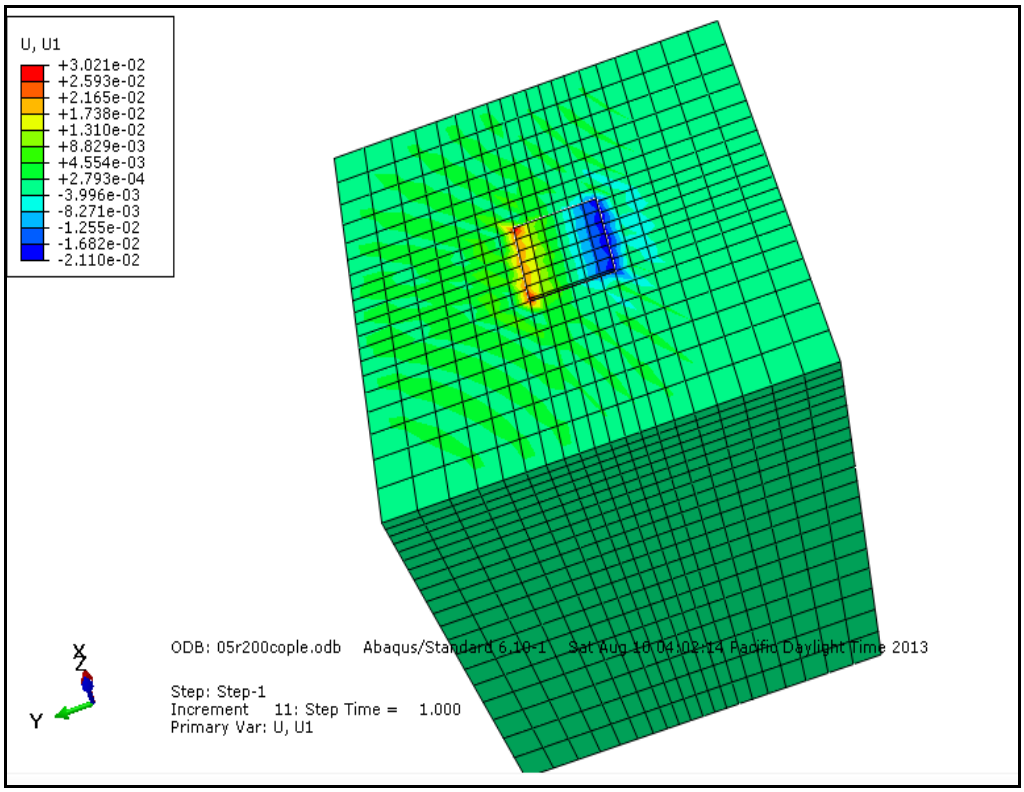


**Figure 15.** Full contours of lateral deflection (m) at raft thickness =0.5 m and F=20 kN.

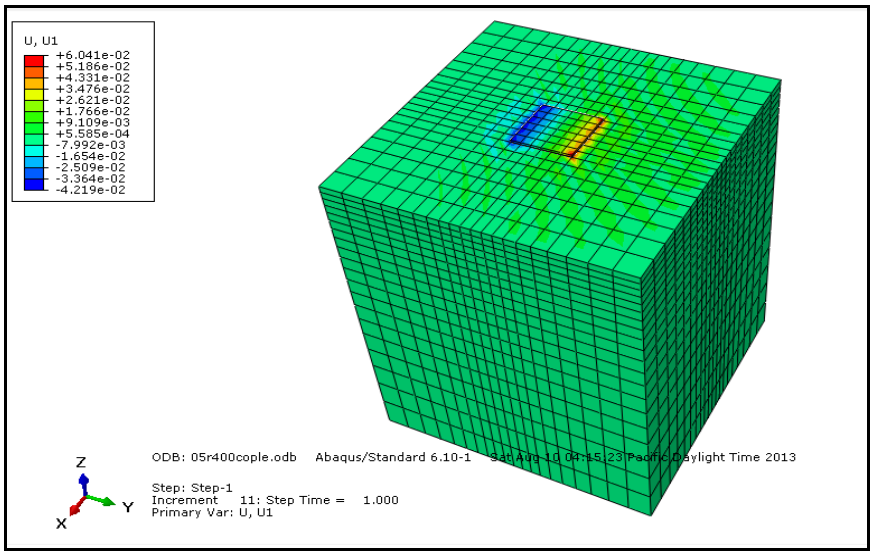


**Figure 16.** Full contours of lateral deflection (m) at raft thickness = 0.5 m and F=40 kN**.**

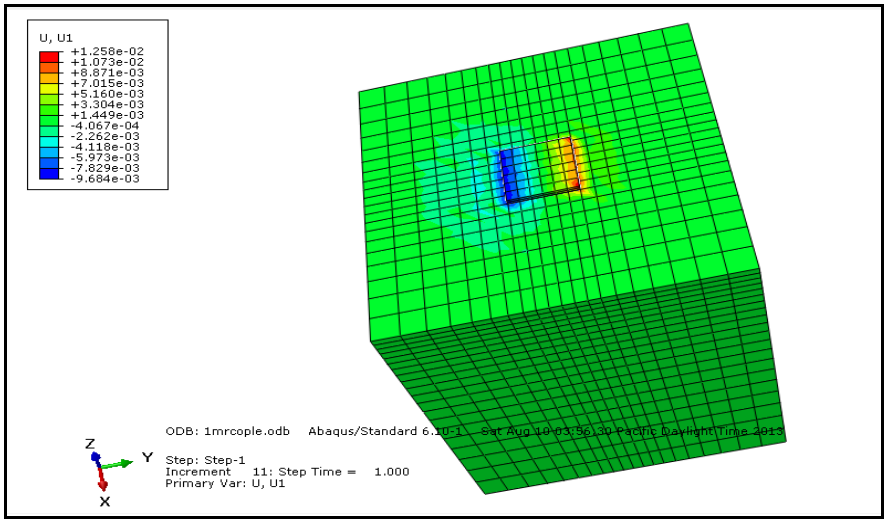


**Figure 17.** Full contours of lateral deflection (m) at raft thickness =1.0 m and F=10 kN.

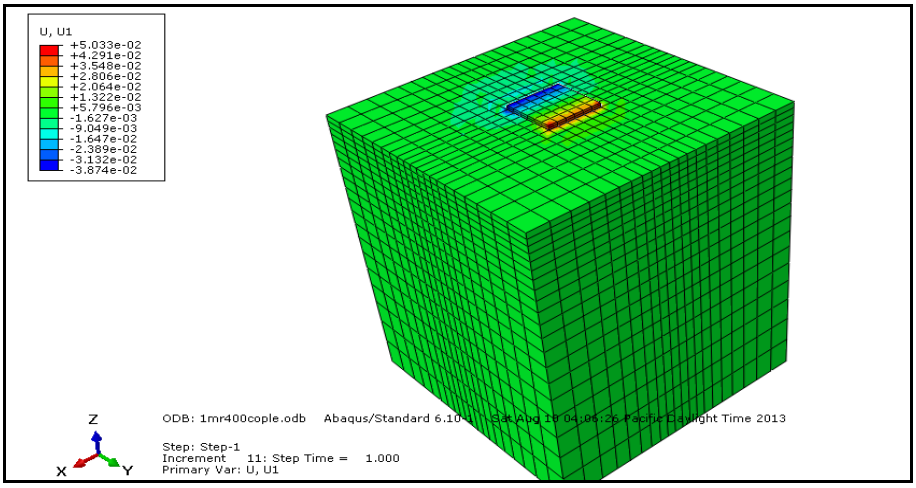


**Figure 18.** Full contours of lateral deflection (m) at raft thickness =1.0 m and F=40 kN.

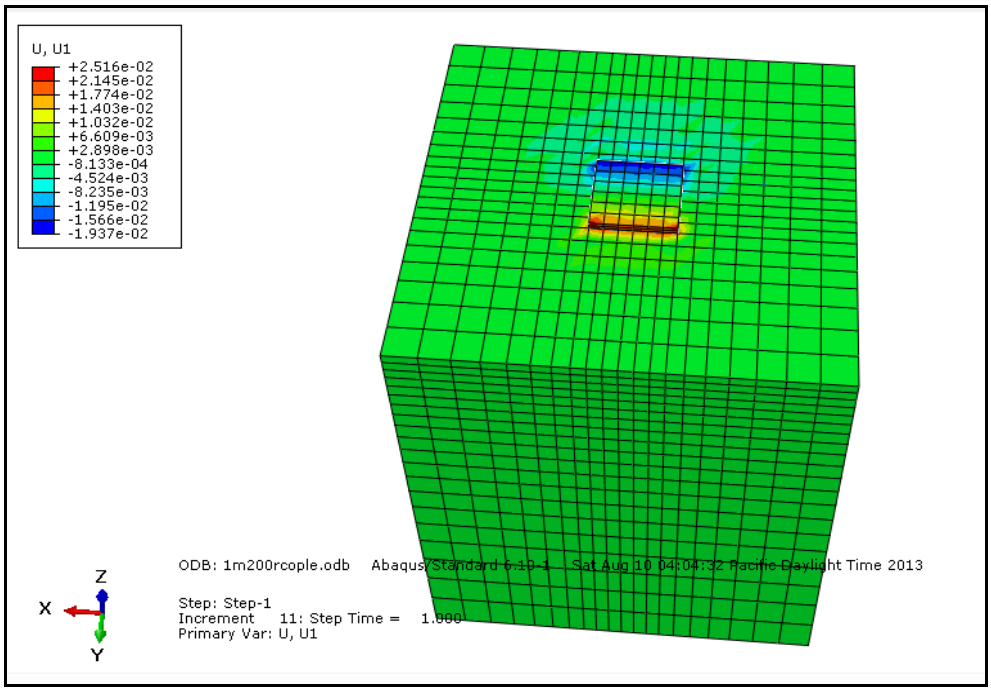


**Figure 19.** Full contours of lateral deflection (m) at raft thickness =1.0 m and F=20 kN**.**

**Table 1.** Properties and dimensions of the raft.

| Property | Value |
|---|---|
| Unit weight of concrete($\gamma_c$ kN/m$^3$) | 24 |
| Elastic modulus of concrete ($E_c$, kN/m$^2$) | 23.5 x 10$^3$ |
| Raft width (w, m) | 12 |
| The thickness of raft (t, m) | 0.5, 1.0 and 1.5 |
| Poisson's ratio of concrete ($v$) | 0.15 |

**Table 2.** Characteristics of sand soil.

| | |
|---|---|
| Relative Density (RD %) | 30 |
| State sand | Loose |
| Angle of friction (Ø°) | 29.0 |
| Cohesion(c, kN/m$^2$) | 0 |
| Poisson's ratio of soil($v$) | 0.3 |
| Modulus of deformation($E_s$, kN/m$^2$) | 10000 |
| (Gs) | 2.65 |
| The dry unit weight of soil ($\gamma_d$, kN/m$^3$) | 15.3 |